10/502332.

3/31/05 -

PCT / IB 03 / 01044

04. 06. 03

REC'D 04 JUN 2003
WIPO PCT

PA 10

THE UNITED STATES OF AMERICA

TO ALL TO WHOM THESE PRESENTS SHALL COME:

UNITED STATES DEPARTMENT OF COMMERCE

United States Patent and Trademark Office

May 27, 2003

THIS IS TO CERTIFY THAT ANNEXED HERETO IS A TRUE COPY FROM THE RECORDS OF THE UNITED STATES PATENT AND TRADEMARK OFFICE OF THOSE PAPERS OF THE BELOW IDENTIFIED PATENT APPLICATION THAT MET THE REQUIREMENTS TO BE GRANTED A FILING DATE UNDER 35 USC 111.

APPLICATION NUMBER: ***60/356,136***
FILING DATE: ***February 14, 2002***

PRIORITY DOCUMENT
SUBMITTED OR TRANSMITTED IN COMPLIANCE WITH RULE 17.1(a) OR (b)

By Authority of the
COMMISSIONER OF PATENTS AND TRADEMARKS

VIELKA BROWN
Certifying Officer

60356136.021402 Prov

PTO/SB/16 (6-95)
Approved for use through 04/11/98. OMB 0651-0037
Patent and Trademark Office, U.S DEPARTMENT OF COMMERCE

02/14/02 J1132 U.S. PTO

PROVISIONAL APPLICATION COVER SHEET

This is a request for filing a PROVISIONAL APPLICATION under 37 CFR § 1.53(b)(2).

Docket Number	1029/00241	Type a plus sign (+) inside this box	+

JC857 U.S. PTO 60/356136 02/14/02

INVENTOR(s)/APPLICANT(s)

LAST NAME	FIRST NAME	MIDDLE INITIAL	RESIDENCE (CITY AND EITHER STATE OR FOREIGN COUNTRY)
Aguado	Enrique		
Nunez-Cruz	Selene		
Miazek	Arkadiusz		
Richelme	Sylvie		
Mura	Anne-Marie		
Richelme	Mireille		
Sainty	Danielle		
He	Hai-Tao		
Malissen	Bernard		
Malissen	Marie		

TITLE OF INVENTION (280 characters max)

SPONTANEOUS EXAGGERATED T HELPER TYPE 2 IMMUNITY IN MICE WITH A POINT MUTATION IN LAT

CORRESPONDENCE ADDRESS

Connolly Bove Lodge & Hutz LLP. 1990 M Street, N.W., Suite 800, Washington

STATE	DC	ZIP CODE	20036-3425	COUNTRY	USA

ENCLOSED APPLICATION PARTS *(check all that apply)*

[XX] Specification — *Number of Pages* [23] — [ ] Small Entity Statement

[XX] Drawing(s) — *Number of Sheets* [8] — [ ] Other (specify) _____

METHOD OF PAYMENT *(check one)*

[ ] A check or money order is enclosed to cover the Provisional filing fees	PROVISIONAL FILING FEE AMOUNT ($)	$160.00
[XX] The Director is hereby authorized to charge the filing fees and credit Deposit Account Number: 22-0185.		

The invention was made by an agency of the United States Government or under a contract with an agency of the United States Government.

[ ] No.

[ ] Yes, the name of the U.S. Government agency and the Government contract number are: _____

Respectfully submitted,

SIGNATURE _____ Date February 14, 2002

TYPED or PRINTED NAME Morris Liss *(if appropriate)* REGISTRATION NO. 24,510

[ ] Additional inventors are being named on separately numbered sheets attached hereto

PROVISIONAL APPLICATION FILING ONLY

BM-18bis/NG
5/11/01

Spontaneous exaggerated T helper type 2 immunity in mice with a point mutation in LAT

Enrique Aguado[1], Selene Nunez-Cruz[1], Arkadiusz Miazek[1], Sylvie Richelme[1], Anne-Marie Mura[1], Mireille Richelme[1], Danielle Sainty[2], Hai-Tao He[1], Bernard Malissen[1*] and Marie Malissen[1].

[1] Centre d'Immunologie de Marseille-Luminy, INSERM-CNRS-Univ.Med., Parc Scientifique de Luminy, 13288 Marseille Cedex 9, France.

[2] Department of Biology, Institut Paoli-Calmettes, 232 Bd Sainte Marguerite, 13009 Marseille, France.

* To whom correspondence should be addressed. E-mail: bernardm@ciml.univ-mrs.fr

LAT (Linker for Activation of T cells) couples the T cell receptor (TCR) to downstream signaling effectors via tyrosines within its cytoplasmic tail. We provide genetic evidence that LAT exerts an unanticipated inhibitory function on the differentiation of CD4 helper T (T_H) cells into T_H2 cells. Mice homozygous for a mutation of a single LAT tyrosine show both an impeded T cell development and a precocious and spontaneous accumulation of polyclonal T_H2 cells which chronically produce large amounts of interleukin 4, 5, 10 and 13. This exaggerated T_H2 differentiation leads in turn to tissue eosinophilia and to the maturation of massive numbers of plasma cells secreting IgE and IgG1 antibodies. Thus, in addition to known positive signaling, LAT appears also essential for establishing inhibitory signals that control T cell homeostasis.

TCR recognize peptide fragments bound to major histocompatibility complex (MHC) molecules and relay this information to the interior of the T cell via adapter proteins. One of these, the adapter LAT, coordinates the assembly of signaling complexes through multiple tyrosine residues within its intracytoplasmic segment (1). Upon TCR-induced phosphorylation, each of these tyrosines manifests some specialization in the signaling proteins it recruits. For instance, mutation of tyrosine 136 (Y136) selectively eliminates binding of phospholipase Cγ1 (PLC-γ1) whereas the simultaneous mutation of Y175, Y195 and Y235 results in loss of binding of downstream adapters Gads and Grb-2 (2-4). During T cell development, the pre-TCR and the αβ TCR control the transition from the double negative (DN) to the double positive (DP) stage, and the transition from the DP to the single positive (SP) stage, respectively. These two molecular sensors of developing T cells share many signaling components with the TCR on mature T cells. In support of this view, mice deficient in LAT ($LAT^{-/-}$), or with a mutation of the four carboxy-terminal tyrosine residues (Y136, Y175, Y195 and Y235) of LAT ($LAT^{4YF/4YF}$) revealed that LAT is essential for the function of the pre-TCR (5,6).

To test in vivo the importance of LAT Y136, we generated knock-in mice with a mutation replacing Y136 with phenylalanine (Y136F). Mice homozygous for the LAT Y136F mutation, hereafter denoted LAT^{Y136F}, were born at expected Mendelian frequencies and their T cells contained levels of LAT proteins similar to wild-type T cells (7). At birth LAT^{Y136F} mice displayed peripheral lymphoid organs of normal size. Beginning at about 3 weeks, however, the spleen and lymph nodes of the mutant mice started to enlarge relative to wild-type littermates, such that by 15 weeks of age, spleen cellularity was approximately 10 times that of wild-type mice (Fig.1 A-C). Despite marked lymphocytic infiltrations in the lung, liver and kidney, homozygotes lived to at least 17 weeks of age, and no chronic intestinal inflammation or tumor formation was observed (8). The effects of the LAT Y136F mutation were only detectable after breeding mice to homozygosity or to mice carrying a null allele of the LAT gene (8).

The thymi of LAT^{Y136F} mice were small and differed from both $LAT^{-/-}$ and $LAT^{4YF/4YF}$ thymi in that they contained DP cells (Fig. 1 and 2). However, these numbers were dramatically reduced when

compared to age-matched wild-type thymi (Fig. 1D and E). After reaching a peak in newborn mice, DP cell numbers decreased and were almost undetectable in mutant mice older than 7 weeks (Fig. 2A). Coincident with this progressive DP cell erosion, discrete populations of SP thymocytes started to dominate the thymus and showed a CD4/CD8 ratio skewed towards CD4 cells. The levels of TCR expressed at the surface of LAT^{Y136F} thymocytes were slightly (DP) or markedly (SP) lower than those observed in wild-type mice (Fig. 2B). The DP thymocytes found in young mutant mice were further distinguished from wild-type DP cells because they lacked CD5 molecules at their surface (Fig. 1F). CD5 is a negative regulator of TCR signaling and its expression increases during T cell development in a manner proportional to the intensity of pre-TCR and TCR signaling (9-11). From these data and the presence of a normal complement of DN cells in LAT^{Y136F} thymi (8), we conclude that the LAT Y136F mutation resulted in a severe but partial impairment of $\alpha\beta$ T cell development, likely due to a selective uncoupling of the pre-TCR from PLC-γ1 (12). In marked constrast, this mutation did not affect detectably the development and maturation of $\gamma\delta$ T cells (Fig. 1E and 2E).

Given the dearth of SP thymocytes found in newborn LAT^{Y136F} mice (Fig. 1A and B), one would expect to detect very few SP cells in secondary lymphoid organs. However, SP cells appeared in the spleen and lymph nodes of LAT^{Y136F} mice with the same kinetics as in wild-type mice, and additionally showed a bias in favor of CD4 cells even more pronounced than that noted in the thymus (Fig. 2C and D). These CD4 cells had a $CD25^{-}$, $CD44^{hi}$, $CD62L^{lo}$, $CD69^{+}$ phenotype similar to activated/memory T cells (Fig. 2F), and expressed low levels of TCR on their surface, an attribute that may in part account for their inability to respond to TCR stimulation in vitro (8). Analysis of DNA content by propidium iodide staining showed that the CD4 populations from wild-type and LAT^{Y136F} mice contained 3.3 and 7.2% of cells in G2/S/M phase of the cell cycle, respectively (8). Moreover, when cultured in medium alone, CD4 T cells purified from LAT^{Y136F} mice showed a dramatically lower rate of spontaneous apoptosis than wild-type CD4 T cells (8). Therefore, the progressive accumulation of CD4 T cells in the periphery of LAT^{Y136F} mice is probably due to both their extended survival and modestly increased proliferation.

A prominent phenotype of the CD4 T cells found in LAT^{Y136F} mice was revealed when we measured their ability to make cytokines. Due to the short half-lives of cytokines and of their transcripts, their analysis generally requires restimulation of T cells in vitro with PMA and ionomycin (12,13). A multiprobe Rnase protection assay detecting levels of transcripts of 9 cytokines showed that CD4 T cells freshly isolated from LAT^{Y136F} mice contained sufficient IL-4 and IL-10 transcripts to allow their detection even without ex vivo restimulation (Fig. 3A). Upon activation by PMA/ionomycin the levels of IL-4 and IL-10 transcripts they contained were further increased, and IL-5, IL-13, and IFN-γ transcripts became readily detectable (Fig. 3B). In marked contrast, wild-type CD4 T cells yielded only the IL-2 and IFN-γ transcripts expected for primary T cells. Analysis of IL-4 production at the single cell level, showed that following a 4 hr activation with PMA/ionomycin, close to 80% of the CD4 T cells isolated from LAT^{Y136F} mice expressed very high levels of IL-4 (Fig. 3C). Consistent with the notion that these CD4 T cells were refractory to TCR stimuli, none of them scored as $IL\text{-}4^+$ in response to TCR cross-linking (Fig. 3C). Thus, LAT^{Y136F} spontaneously developed a high frequency of T_H2 cells. In the case of wild-type CD4 T cells, T_H2 polarization of such magnitude is only achieved following prolonged antigenic stimulation in the presence of IL-4 (14).

Light scatter analysis of thymic and lymph node cells from LAT^{Y136F} mice older than 4 weeks revealed a unique cell population that was almost absent from age-matched wild-type mice, and showed both an intermediate forward scatter and a high side scatter (Fig. 2A and C). Based on several of criteria, we identified these cells as eosinophils (7). Minute numbers of eosinophils normally reside in wild-type thymi (15,16), and their augmentation in LAT^{Y136F} thymi may primarily result from an intrinsic expression of LAT Y136F molecules. However, LAT transcripts were undetectable in eosinophils purified from LAT^{Y136F} mice (7), suggesting that the thymic and lymph node eosinophilia they manifest result from the production of IL-5 by the abnormal CD4 cells present in these mutant mice. Along this line, most of the CD4 thymocytes found in LAT^{Y136F} mice older than 4 weeks had a phenotype ($CD44^{hi}$, $CD62L^{lo}$, $CD69^+$, and HSA^-) distinct from that expected for genuine CD4 SP thymocytes, but closely resembling that of the abnormal peripheral CD4 cells. Provided that the latter cells effectively recirculated to the thymus, the IL-

5 and IL-13 cytokines they produced in situ are likely to be primarily responsible for the progressive disappearance of DP thymocytes, and the thymic eosinophilia (17,18).

Secondary lymphoid organs of 6-week old LAT^{Y136F} mice contained 7 to 10 times more B cells than their wild-type counterparts. Thus, the splenomegaly and generalized lymphadenopathy that developed in young LAT^{Y136F} mice can be mostly accounted for by cells belonging to the T and B cell lineages. Over 90% of the mature B cells found in the spleen and lymph nodes of 6-week old wild type littermates had a resting phenotype (B220^{high}, MHC class II^{+}, IgM^{+}, IgD^{+}; Fig. 4A). In marked contrast, only 25% of the B cells found in the enlarged secondary lymphoid organs of age-matched LAT^{Y136F} littermates showed a resting phenotype. Among the remaining B cells, 25% showed an hyperactivated phenotype (B220^{high}, MHC class II ^{high}, IgD^{-}), and 50% expressed a phenotype typical of antibody-producing cells (B220^{low}, MHC class II^{+}, IgD^{-}, IgM^{-}, CD44^{high}; Fig. 4A). Coincident with the presence of these latter cells, serum IgG1 concentrations were elevated approximately 200 times compared to wild-type mice, whereas those of IgE were elevated 2500 to 10000 times (Fig. 4B). In contrast, the levels of the other Ig isotypes did not differ significantly from those of wild-type serum. In support of a polyclonal hypergammaglobulinemia G1 and E, the concentrations of kappa and lambda light chains were both markedly augmented in the serum of LAT^{Y136F} mice (Fig. 4B). Notably, IgE and IgG1 antibody concentrations reached a plateau as early as 5 weeks of age (Fig. 4 C), the values of which exceeded the extraordinarily large amounts of IgE and IgG1 previously reported for mice deprived of NFATc2 and NFATc3 transcription factors (19). Given that B cells do not express LAT proteins (1), and considering that isotype switching to IgE and IgG1 is highly dependent on the presence of IL-4 and IL-13 (17), the overproduction of IgE and IgG1 noted in LAT^{Y136F} mice is probably secondary to the presence of an abnormally high frequency of T_H2 effectors.

The close temporal relationship existing between the appearance of the first peripheral CD4 T cells and the earliest signs of eosinophilia and hypergammaglobulinemia E and G1 suggested that CD4 cells were primarily responsible for the disorders documented in LAT^{Y136F} mice. We tested this hypothesis by genetically ablating the whole T cell lineage or some of its subsets. We first used a mutation (CD3-$\varepsilon^{\Delta 5}$;

20) that blocks the progression beyond the DN stage and thus prevents the development of all mature T cells . Consistent with the absence of detectable LAT transcripts in B cells and eosinophils, we showed that the introduction of the LAT^{Y136F} genotype was without detectable effect on the B cells and eosinophils that are normally present in CD3-$\varepsilon^{\Delta 5}$ mice (7). Moreover, the cellularity and composition of the DN cell population found in CD3-$\varepsilon^{\Delta 5}$ x LAT^{Y136F} mice were comparable to those of wild-type mice, indicating that the effects of the LAT Y136F mutation become manifest only at the DN to DP transition. By breeding the LAT^{Y136F} mice to β2-microglobulin-deficient mice, we directly assessed the role of the residual CD8 T cells found in LAT^{Y136F}, and showed that they were dispensable for the development of the disorders (8). In contrast, the absence of CD4 T cells in mice genetically deficient for both MHC class I and class II molecules (MHC KO), protected them from the pathological effects of the LAT Y136F mutation (7). These data indicate that the CD4 T cells found in LAT^{Y136F} mice are required for the development of the pathology.

When compared to those present in the thymus of MHC-deficient mice, the DP thymocytes found in mice of LAT Y^{136F} x MHC KO genotype were $CD5^-$, and their numbers although reduced 20 times were stable over time (7). Because they were obtained in a genetic background where noxious CD4 T cells cannot interfere with developing DN and DP thymocytes, these results established that the negative impact exerted by the LAT Y136F mutation on the DN to DP transition is cell autonomous, and conversely, that it is the CD4 T cells that were responsible for the progressive erosion of the DP cell compartment. The total absence of CD5 molecules at the surface of the few DP thymocytes that develop in both LAT^{Y136F} and LAT^{Y136F} x MHC KO mice may be part of positive tuning mechanisms allowing the pre-TCR to adapt to the lowered signalling potential of the LAT Y136F molecules (9-11).

The absence of pathologic CD4 T cells in LAT^{Y136F} mice deprived of MHC class II molecules, suggests that in LAT^{Y136F} mice these cells went through a thymic selection process involving MHC class II molecules. Consistent with this notion, these cells used a diverse repertoire of Vα and Vβ segments (8). These two attributes readily distinguish them from CD1-d restricted T cells. Given that these CD4 T cells were anergic when challenged via their TCR in vitro, we converted them into T cell hybridomas to

determine the specificity of their TCR. Due to the recessive character of the LAT Y136F mutation, the coexpression of wild-type and LAT Y136F molecules in the resulting hybridomas did not prevent the production of IL-2 following TCR engagement. Remarkably, all the hybridomas derived from LAT^{Y136F} CD4 T cells reacted with syngeneic spleen cells (Table 1), whereas control T cell hydridomas derived from wild-type CD4 T cells showed no autoreactivity (8). Notably, these two series of hybridomas expressed comparable levels of TCR at their surface, and used an heterogeneous set of Vβ segments (8). Six out of the seven hybridomas derived from LAT^{Y136F} mice were specific for syngenic MHC class II molecules, while the seventh showed an additional cross-reactivity toward MHC class I molecules (Table 1). Such unexpected reactivity against self-MHC molecules may result from inadequate negative selection and account for the exaggerated help provided to B cells in vivo. Alternatively, the TCR expressed on LAT^{Y136F} CD4 T cells may have been appropriately calibrated in relation to the LAT^{Y136F} context, and it is only after introducing them in T hybridomas, and thus artificially increasing both their surface density and output, that they started displaying a reactivity toward self-MHC class II molecules. According to this last view, the polyclonal hypergammaglobulinemia E and G1 found in LAT^{Y136F} mice may plausibly be due to non cognate interactions between B cells and aberrant T cells overproducing IL-4 in a chronic manner (21,22).

LAT^{Y136F} mice showed both a markedly impeded sequence of T cell development and a massive accumulation of T_H2 effectors in the periphery. This paradoxical phenotype can be accounted for if residue Y136 is capable of activating both a positive and a negative-feedback loops, and if in mature CD4 T cells, ablation of the negative-feedback loop does not lead to compensatory adjustments. According to this postulated dual role, Y136 of LAT may contribute to turn off the signaling pathways activated at the time of positive selection, or to keep in check the low-level TCR signaling mature T cells require to survive in the periphery (23). Once this feedback attenuation function is relieved as in LAT^{Y136F} mice, a persistent signaling state develops in mature T cells, and leads, for reasons that have yet to be defined, to the selective differentiation and accumulation of T_H2 cells which are locked into a chronic production of

IL-4, -5, -10 and -13. This outcome distinguishes LAT^{Y136F} mice from lck- or CD3-ζ/η-deficient strains which present a global diminution of TCR signaling capacity (24). The early onset of the LAT Y136-triggered disorders (serum levels of IgE and IgG1 are already increased as early as 3 weeks of age, Fig. 4C), distinguishes them from the T_H2-type disease that develop in Stra 13-deficient mice (25). The LAT^{Y136F} mice differ also from other mouse strains with T cell lymphoproliferative disorders (CTLA-4-deficient, IL2Rα-deficient, lpr and gld strains ; 26), but strikingly resemble mice deprived of NFATc2 and NFATc3 transcription factors (19). The combined absence of NFATc2 and NFATc3 probably disrupted the balance among NFAT family members and lowered the threshold TCR-initiated signals have to overcome to trigger the import of NFATc1 into the nucleus and the transactivation of the IL-4 gene. Therefore, presumably unleashing signal propagation at two distinct levels of the TCR transduction cassette, the LAT^{Y136F} and NFATc2/c3 mutations triggered a runaway feedback pathway that resulted in similar effects on lymphoid homeostasis and T_H2 differentiation. Despite these striking similarities, the NFATc2/c3-deficient and LAT^{Y136F} mice differ however, in that the thymi of the former were normal and their peripheral T cells hyperresponsive to TCR-mediated signals. The negative role postulated for the LAT Y136 residue can be reconciled with the recessive nature of the LAT Y136F mutation provided that in heterozygous mice the aberrant signals delivered by LAT Y136F molecules are blunted by signals emanating from the wild-type LAT molecules that colocalize in the supramolecular activation clusters found at the junction between T cells and antigen-presenting cells. Despite being strikingly absent on LAT^{Y136F} DP thymocytes, CD5 molecules were however readily detectable on their direct progeny (Fig.1F). Given the ability of CD5 to dynamically tune TCR signalling (9,11), this very late induction can be interpreted as a failed attempt to desensitize the chronically activated CD4 T cells that develop in LAT^{Y136F} mice. Whether other cell types known to express LAT (platelets, natural killer cells, and mast cells; 1) are affected by the LATY136 remains to be determined.

Finally, the pathology developed by LAT^{Y136F} mice is reminiscent of the clinical features manifested by patients suffering from the idiopathic hypereosinophilic syndrome (27,28), raising the

possibility that they have inherited a null allele of LAT and developed clonal populations of pathogenic T_H2-type lymphocytes as a result of somatic missense mutations at position 136 of the active LAT allele. Although the underlying mechanisms by which the LAT^{Y136F} mutation impacts on T cell development and differentiation remain to be fully defined, our results reveal that restricting LAT to only a subset of its docking functions affects the decision of T_H cells to differentiate into T_H1 or T_H2 effectors. It is therefore possible that in a physiological context, the differential phosphorylation of some of the tyrosines found in LAT influences CD4 T_H cell differentiation.

References and Notes

1. W. Zhang, J. Sloan-Lancaster, J. Kitchen, R.P. Trible, L.E. Samelson, *Cell* **92**, 83 (1998).

2. J. Lin, A. Weiss, *J. Biol. Chem.* **276**, 29588 (2001).

3. P.E. Paz, S. Wang, H. Clarke, X. Lu, D. Stokoe, A. Abo, *Biochem. J.* **356**, 461 (2001).

4. W. Zhang *et al.*, *J. Biol. Chem.* **275**, 23355 (2000).

5. W. Zhang *et al.*, *Immunity* **10**, 323 (1999).

6. C.L. Sommers *et al.*, *J. Exp. Med.* **194**, 135 (2001).

7. See Supplementary information

8. M. Malissen, unpublished observations

9. A. Tarakhovsky *et al.*, *Science* **269**, 535 (1995).

10. H.S. Azzam *et al.*, *J. Exp. Med.* **188**, 2301 (1998).

11. K. Smith *et al.*, *J. Exp. Med.* **194**, 1253 (2001).

12. C.L. Sommers et al., submitted as a companion manuscript.

13. M. Mohrs, K. Shinkai, K. Mohrs, R.M. Locksley, *Immunity* **15**, 303 (2001).

14. E. Murphy *et al.*, *J. Exp. Med.* **183**, 901 (1996).

15. A.N. Matthews *et al.*, *Proc. Natl. Acad. Sci. USA* **95**, 6273 (1998).

16. M. Throsby, A. Herbelin, J.-M. Pléau, M. Dardenne, *J. Immunol.* **165**, 1965 (2000).

17. C.L. Emson, S.E. Bell, A. Jones, W. Wisden, A.N.J. McKenzie, *J. Exp. Med.* **188**, 399 (1998).

18. M. Goldman, A. LeMoine, M. Braun, V. Flamand, D. Abramowicz, *Trends in Immunol.* **22**, 247 (2001).

19. A.M. Ranger, M. Oukka, J. Rengaraja, L.H. Glimcher, *Immunity*, **9**, 627 (1998).

20. M. Malissen *et al.*, *EMBO J.*, **14**, 4641 (1995).

21. K.J. Erb *et al.*, *J. Exp. Med.*, **185**, 329 (1997).

22. L.C. Foote, A. Marshak-Rothstein, T.L. Rothstein, *J. Exp. Med.*, **187**, 847 (1998).

23. A.W. Goldrath, M.J. Bevan, *Nature*, **402**, 255 (1999).

24. B. Malissen, L. Ardouin, S.-Y. Lin, A. Gillet, M. Malissen, *Adv. Immunol.*, **72**, 103 (1999).

25. H. Sun, B. Lu, R.-Q. Li, R.A. Flavell, R. Taneja, *Nat. Immunol.*, **2**, 1040 (2001).

26. L.Van Parijs, A.K. Abbas, *Science*, **280**, 243 (1998).

27. H.-U. Simon, S.G. Plotz, R. Dummer, K. Blaser, *New Engl. J. Med.*, **341**, 1112 (1999).

28. F. Roufosse *et al.*, *British J. Haematol.*, **109**, 540 (2000).

29. We thank S. Guerder, P. Naquet, P. Golstein, R. Guinamard G. Millon, D. Emilie, and L. Leserman, for discussion, B. Ryffel and Cecile Fremont for histological analysis, A. Gillet, N. Brun and M. Barad, for advices and N. Guglietta for editing the manuscript. Supported by CNRS, INSERM, ARC/ARECA, AFM, and the European Communities (project QLG1-CT1999-00202). E.A. and A.M. were supported by fellowships from the European Communities, the FRM, and the HFSPO. S.N.C. was supported by a France-Mexico exchange fellowship (SFERE-CONACYT).

Table 1. $CD4^+$ hybridomas derived from LAT^{Y136} mice are self-reactive and recognize β2m- or MHC class II-dependent ligands.
Hybridomas were cultured with irradiated splenocytes isolated from H-2^b mice of the specified genotype. Cultures were for 20 h, at which time supernatant were assayed on the IL-2 dependent line CTL-L. Growth of the CTL-L was estimated by [^{3}H] thymidine incorporation. Mean values for duplicate samples are given.

	IL-2 secreted (thymidine incorporation) in response to			
Responder hybridomas	$\beta2m^+$, II^+ splenocytes	$\beta2m^o$, II^+ splenocytes	$\beta2m^+$, II^o splenocytes	$\beta2m^o$, II^o splenocytes
3	13,193	13,095	583	568
15	5,787	4,770	174	226
21	8,450	7,549	207	375
28	13,483	14,319	349	322
39	12,531	13,832	682	467
72	9,238	9,739	538	542
22	13,070	12,088	6,893	715

Figure Legends

Figure 1. Impeded fetal thymic ontogeny and aberrant growth of the thymus and secondary lymphoid organs in LAT^{Y136F} mice. **(A through C)** Aberrant growth of peripheral lymphoid organs in LAT^{Y136F} mice. Shown are the thymus (A), the spleen (B) and the lymph nodes (C, inguinal and mesenteric), removed from wild-type littermate control and 7-week old LAT^{Y136F} mice. **(D)** CD4/CD8 staining profiles of total thymocytes from wild-type and from LAT^{Y136F} mice at different ages of embryonic life and at 1 and 2 weeks of age. The percentages of cells within each quadrant is indicated. **(E)** Absolute number of total thymocytes, DP cells, TCR$\alpha\beta^{hi}$ cells and $\gamma\delta$ T cells found in LAT^{Y136F} and wild-type thymi are represented at the indicated ages. **(F)** Comparison of the levels of CD5 and HSA on DP, CD4 SP, and CD8 SP thymocytes from 6 week-old mice expressing wild-type LAT or LAT Y136F molecules. Boxes define the specified subpopulations. The eosinophils found in LAT^{Y136F} thymi were excluded from the analysis on the basis of their unique forward and side scatters.

Figure 2. Phenotypic analysis of thymocytes and T cells from wild-type and LAT^{Y136F} mice. **(A)** Light scatter analysis and CD4/CD8 staining profiles of total thymocytes from wild-type and from LAT^{Y136F} mice at 5 and 7 weeks of age. The percentages of cells within each gate are indicated. **(B)** Comparison of the levels of CD3 on DP, CD4 SP, and CD8 SP thymocytes from 6 week-old mice expressing wild-type LAT or LAT Y136F molecules. Shaded areas correspond to staining with negative control antibodies and the solid lines to staining with the specified antibodies. **(C)** Light scatter analysis and CD4/CD8 staining profiles of total lymph node cells from wild-type and from LAT^{Y136F} mice at 6 weeks of age. **(D)** CD4/CD8 staining profiles of spleen cells from wild-type and from LAT^{Y136F} mice at 6 weeks of age. **(C)** Comparison of the levels of CD3, CD69, CD62L, CD44 and CD95 on CD4$^+$ cells from 6 week-old mice expressing wild-type LAT or LAT Y136F molecules. **(E)** $\gamma\delta$ T cells develop in LAT^{Y136F} mice and express normal levels of TCR $\gamma\delta$ complexes at their surface. Thymocytes and lymph node cells isolated from 6-week old wild-type and LAT^{Y136F} mice were analyzed by flow cytometry for the expression of TCR$\gamma\delta$ versus CD3-ε. Windows were set on TCR$\gamma\delta^+$

CD3-ε^+ and TCR$\gamma\delta^-$ CD3-$\varepsilon^{low\ to\ high}$ subpopulations. The eosinophils present in the thymi and lymph nodes of LAT^{Y136F} mice were excluded from the analysis on the basis of their forward and side scatters. When averaged from three experiments, the absolute numbers of γδ T cells per thymus were 0.9×10^6 and 1.3×10^6 for wild-type and LAT^{Y136F} littermates, respectively.

Figure 3. Constitutive type-2 cytokine production in CD4 T cells freshly isolated from LAT^{Y136F} peripheral lymphoid organs. **(A).** Analysis of the cytokine transcripts expressed in ex vivo CD4 T cells isolated from the spleen of wild-type (lane 3) and LAT^{Y136F} (lane 4) mice. Total RNA was analyzed by a multiprobe ribonuclease protection assay using a MCK1 RiboQuant mouse template set. The autoradiogram also shows the MCK1-probe set not treated with RNase (lane 1) and a control sample provided by the supplier (lane 2). The identity of the various protected bands is indicated on the right. **(B)** Analysis of the cytokine transcripts expressed in CD4 T cells isolated from wild-type- (lane 2) and LAT^{Y136F} (lane 3) mice following stimulation by PMA/ionomycin for 15 hr. Lane 1 corresponds to wild-type CD4 T cells that were grown under T_H2 polarizing conditions. Samples were processed as described in (A). **(C)** IL-2, IL-4, IL-5 and IFNγ production analyzed at the single cell level. Ex vivo CD4 T cells purified from wild-type and from LAT^{Y136F} lymph nodes were cultured for 4 hr in the presence of monensin to trap cytokine in the endoplasmic reticulum. During the culture period, cells were either left unstimulated or stimulated with an anti-CD3-ε antibody, or with PMA/ionomycin. At the end of the culture, cells were processed for intracellular staining. Numbers indicate percentages of cells in the respective gates.

Figure 4. Hyperactivated B lymphocytes and massive serum levels of IgE and IgG1 antibodies in unimmunized LAT^{Y136F} mice. **(A)** Dot plots show the B220 vs MHC class II profiles of wild-type and LAT^{Y136F} B cells. Boxes define $B220^{low}$ and $B220^{high}$ B cell populations. Data are representative of 4 mice aged 6-7 weeks. **(B)** Sera from 6-week old wild-type and LAT^{Y136F} mice were subjected to a tenfold serial dilution and the titres of the specified Ig isotypes determined by ELISA. Data are representative of 3 mice. **(C)** Early appearance of IgE and IgG1 in the sera of LAT^{Y136F} mice. The concentrations of IgE and IgG1 found in individual mice were plotted on a logarithmic scale.

Suplementary Material

Mice

Mice were maintained in our specific pathogen-free animal facility. Fetal thymi were analyzed between days 14.5 and day 19.5 of gestation (referred to as E14.5, E19.5, etc...). Recombination activating gene (RAG)-1- and TCRα- deficient mice were originally obtained from E. Spanopolou (1) and M.J. Owen (2), respectively CD3-ε deficient mice were obtained as previously described (CD3-$\varepsilon^{\Delta 5}$; 3). Mice lacking both MHC class I and MHC class II molecules were derived by interbreeding β2-microglobulin-deficient mice (4) and MHC class II-deficient mice (5).

LAT Y136F mutation.

LAT genomic clones were isolated from a 129/Ola phage library. After establishing the nucleotide sequence and the exon-intron structure of the LAT gene, the tyrosine residue found at position 136 and encoded by exon 7 was mutated to phenylalanine. Mutagenesis was performed on a 1717-bp Eco RI-Xba I fragment encompassing part of exon 5, exons 6, 7 and 8. In addition to the intended mutation, a new Bgl II restriction enzyme cleavage site was introduced in the intron 3' of exon 7 to accomodate the LoxP-flanked neo^r gene and facilitate subsequent identification of LAT Y136F mutant mice. Finally, the targeting construct was extended to give 1.7 kb and 4.8 kb of homologous sequences 5' and 3' of the EcoRI-XbaI fragment, respectively (see supplemental Fig. 1A). After electroporation of CK35 129/SV ES cells (6), and selection in G418, colonies were screened for homologous recombination by Southern blot analysis. The 5' single-copy probe is a 0.9-kb Bgl II-Xba I fragment isolated from a LAT genomic clone. When tested on Bgl II-digested DNA, the 5' probe hybridizes either to a 8.5 kb wild-type fragment or to a 4.5 kb recombinant fragment. Homologous recombination events at the 3' side were screened by long range PCR. Homologous recombinant ES clones were further checked for the presence of the intended mutation by sequencing the genomic segment corresponding to exon 7. Finally, a neo probe was used to ensure that adventitious non-homologous recombination events had not occurred in the selected clones.

Production of mutant mice.

Mutant ES cells were injected into Balb/c blastocysts. Two LAT^{Y136F} recombinant ES cell clones were found capable of germline transmission. The two mutant mouse lines were first bred to Deleter mice (7) to eliminate the Lox P-flanked neomycin cassette, and intercrossed to produce homozygous mutant mice. The two independently-derived mutant lines showed indistinguishable phenotype. To confirm that the LAT Y136F mutation had been genuinely introduced, LAT transcripts were cloned by reverse transcription and PCR amplification from the thymus of the mutated mice, and the presence of the intended mutation confirmed by DNA sequence analysis. Screening of mice for the presence of the LAT Y136F mutation was performed by PCR using the following pairs of oligonucleotides: c : 5'-GTGGCAAGCTACGAGAACCAGGGT-3' ; d : 5'-GACGAAGGAGCAAAGGTGGAAGGA-3'. The single Lox P site remaining in the LAT^{Y136F} allele after deletion of the neo^r resulted in an amplified PCR product 140 bp-longer than the 510 bp-long fragment amplified from the wild-type LAT allele.

Purification of $CD4^+$ T cells and eosinophils.

Lymph node and spleen cells from several mice were pooled and the $CD4^+$ cells purified using a high gradient magnetic cell separation system (8). Eosinophils were sorted on a FACSvantage on the basis of their FSC^{high}, HSA^+, and $CD11b^+$ phenotype.

Preparation of T cell hybridomas.

Purified $CD4^+$ T cells (>96% purity) were activated with a combination of PMA (5ng/ml, Sigma) and ionomycin (250 ng/ml, Sigma). After 18 hours at 37°C, cells were fused to BW^- cells, a variant of the BW5147 thymoma deprived of functional TCR α and β chain genes (9), and the resulting T cell hybridomas selected as previously described (10).

Stimulation of T cell hybridomas.

In brief, 0.25 ml microcultures were prepared containing 10^5 responding cells and 10^6 irradiated (20 Gy) splenocytes. For stimulation with the anti-CD3-ε antibody 2C11, the bottom of microtiter wells was precoated with 50µl of a 10µg/ml solution of antibody. Cultures were for 20h, at which time

culture supernatants were harvested and assayed for the level of IL-2 using the IL-2-dependent T cell line CTL-L. The amount of [^{3}H] thymidine incorporated into CTL-L cells was measured by direct β counting.

Antibodies and flow cytometric analysis.

Before staining, cells were preincubated on ice for at least 10 min with polyclonal mouse and rat Ig to block Fc receptors. Flow cytometric analysis was performed as described previously (3). All the antibodies were from BD Pharmingen except the anti-CCR3 antibody that was purchased from R&D.

Staining for intracellular cytokines.

Before intracellular cytokine staining, cells (1.5 x 10^6) were cultured for 4 h in the presence of monensin (GolgiStop; BD PharMingen) at a final concentration of 2 μM. Cells were then immediately placed on ice, washed, resuspended in PBS 1X, 1% FCS, 0.90% sodium azide, and stained with an APC-conjugated anti-CD4 antibody. For intracellular cytokine staining, cells were first fixed using the cytofix/cytoperm kit (BD PharMingen). Each cell sample was subsequently split into aliquots that were separately stained with (1) a combination of FITC-conjugated anti-IFN-γ and PE-conjugated anti-IL-2 antibodies, (2) a combination of FITC-conjugated anti-IL-5 and PE-conjugated anti-IL-4 antibodies, and (3) a combination of fluorochrome-conjugated and isotype-matched negative control Ig (BD PharMingen). After a final wash, $CD4^+$ cells (10^4) were analyzed on a FACSCalibur™ flow cytometer after gating out dead cells using forward and side scatters.

RNase protection assay.

For multiplex cytokine transcript analysis, total cellular RNA was isolated from the specified cells using TRIzol (GIBCO-BRL Life Technologies) and analyzed by ribonuclease protection assay using an MCK-1 RiboQuant custom mouse template set (BD Pharmingen). Briefly, ^{32}P-labeled riboprobes were mixed with 10 μg of RNA, incubated at 56°C for 12 to 16 hours, and then treated with a mixture of RNases A and T1 and proteinase K. Rnase-protected ^{32}P-labeled RNA fragments

were separated on denaturing polyacrylamide gels and the intensity of the bands evaluated with a Fuji imaging plate system.

SDS-PAGE and Immunoblotting.

For Western blot analysis of LAT expression, cells were lysed in Triton X-100 lysis buffer (25mM Hepes, pH 7.4; 150 nm NaCl; 1.5 mM $MgCl_2$; 0.2 mM EDTA; and 1X complete protease inhibitors, Roche) for 30 min on ice at a concentration of 1 x 10^7 cells/ml. Nuclei were removed by centrifugation at 12000 x g for 10 min at 4°C. Cell lysates were analyzed by gel eletrophoresis using SDS-PAGE, and western blotting performed with a rabbit anti-LAT serum (Upstate Laboratories).

Determination of serum isotype-specific immunoglobulin levels.

The titres of polyclonal IgM, IgG1, IgG2a, IgG2b, IgG3 and IgA antibodies and κ and λ light chains were determined using isotype-specific ELISA (Southern Biotechnology). The concentrations of IgG 1 and IgE were determined by comparing test sample dilution series values with isotype control standards.

RNA-PCR amplification.

RNA-PCR amplification was performed on total RNA as previously described (11). The sequences of the primers used in Supplemental Figure 2 were :

LAT: 5'-GATTGGCTCATGGGGATCACGTG-3',

NEO: 5'-CGCACGGGTGTTGGGTCGTTTG-3',

MBP-1: 5'-GAGCGTCTGCTCTTCATCTGA-3',

MBP-2: 5'-CACTGAAACTGTGAATGGAGGC-3',

CCR3-1 : 5'-ATGGCATTCAACACAGATGAAATC-3',

CCR3-2: 5'-ACTAAAACACCACAGAGATTTCTTGCT-3',

Thy-1-1 : 5'-TGGACTGCCGCCATGAGAAT-3',

Thy-1-2 : 5'-TCACAGAGAAATGAAGTCCAG-3',

actin-1: 5'-GACTCCGGTGACGGGGTCACC-3', and

actin-2: 5'-CACGATGGAGGGGCCGGACTC-3'.

References

1. E. Spanopoulou *et al., Genes Dev.* **8**, 1030 (1994).

2. K.L. Philpott *et al., Science 256*, 1448 (1992).

3. M. Malissen *et al., Embo J.* **14**, 4641 (1995).

4. B.H. Koller, P. Marrack, J.W Kappler and O. Smithies, *Science* **248**, 1227 (1990).

5. D. Cosgrove *et al., Cell* **66**, 1051 (1991).

6. C. Kress, S. Vandormael-Pournin, P. Baldacci, M. Cohen-Tannoudji, C. Babinet, *Mamm. Genome* **9**, 998 (1998).

7. F. Schwenk, U. Baron, K. Rajewsky, *Nucl. Acids. Res.* **23**, 5080 (1995).

8. S. Miltenyi, W. Müller, W. Weichel, A. Radbruch, *Cytometry* **11**, 231 (1990).

9. J. White *et al., J. Immunol.* **143**, 1822 (1989).

10. S.-Y. Lin, L. Ardouin, A. Gillet, M. Malissen, B. Malissen, *J. Exp. Med.* **185**, 707 (1997).

Supplemental Figure 1. Generation and identification of LAT Y136F knock-in mice. (A) Schematics of LAT Y136F knock-in strategy. (1) Partial restriction map of the wild-type LAT gene. Exons are shown as filled boxes. The restriction sites are: Bg, Bgl II and Xb, Xba I. (2) Targeting vector used for the introduction of the LAT Y136F mutation. The codon present in exon 7 and corresponding to residue Y136 was mutated to phenylalanine, and a novel Bgl II site simultaneously introduced in the intron 3' of exon 7 to facilitate the insertion of the loxP-flanked neo^r gene and to tag the LAT Y136F mutation. Open boxes correspond to the thymidine kinase expression cassette (TK), to the lox P-flanked neo^r gene, and to the pBluescript II KS^+ vector (pBS). Lox P sites are shown as filled triangles. (3) Structure of the targeted allele following homologous recombination. (4) Final structure of the targeted allele after removal of the neo^r gene via Cre-mediated recombination. The 5' single-copy probe used to verify 5' targeting events is indicated and the position of the PCR primers used to verify the presence of appropriate 3' targeting events indicated by arrows. **(B)** Southern blot analysis of the two recombinant ES cell clones that gave germline transmission. DNA was digested with Bgl II and hybridized with the 5' single-copy probe. **(C).** Western blot analysis of LAT proteins in $CD4^+$ T cells isolated from wild-type (wt) and LAT^{Y136F} mice. Cell lysates were analyzed by Western blot using anti-LAT rabbit antiserum. The blot was stripped and reblotted for Thy-1.

Supplemental Figure 2. Eosinophilia in 6-week old LAT^{Y136F} thymi and peripheral lymphoid organs (A). The upper panel dot plot shows the position of the gate that was set to include thymic cells with an intermediate forward scatter (FSC) and a high side scatter (SSC). Lower panels correspond to single color histograms of gated cells after staining with anti-CD11b, anti-CD11c, anti-MHC class II, anti-HSA, anti-CD44, and anti-CCR3 antibodies. When averaged from four experiments using window setting similar to the one shown in this figure, the percentage and absolute numbers of eosinophils per 6-week old LAT^{Y136F} thymus, were 13% and 3.1 x 10^6, respectively. **(B)** Eosinophils sorted from 6-week old LAT^{Y136F} lymph nodes on the basis of their SSC^{hi}, $CD11b^+$ and HSA^+ phenotype were analyzed by cytospin and stained with hematoxylin and eosin (magnifications 160x and 1000x). **(C)** RNA-PCR analysis of LAT, CCR3, and MBP expression in NIH 3T3 fibroblasts (lane 1), RAG-1-deficient thymocytes (lane 2), LAT-deficient thymocytes (lane 3), and in eosinophils sorted from 6-week old LAT^{Y136F} thymi (lane 4) and lymph nodes (lane 5) on the basis of their SSC^{hi},

CD11b^{+} and HSA^{+} phenotype. To evaluate whether LAT transcripts were expressed in thymic eosinophils sorted from LAT^{Y136F}, thymocytes from mice deficient in either RAG-1 or LAT were used as positive and negative controls, respectively. Total RNA was reverse transcribed and the resulting cDNAs amplified with 30 cycles of PCR using pairs of specific primers. Each amplified product was run on agarose gel and revealed by ethidium bromide staining. Control PCR were set up in parallel using a pair of primers specific for the actin gene to control for the quantity and quality of RNA in each sample. The lack of contaminating T cells in sorted eosinophils was corroborated by PCR with a pair of primers specific for Thy-1 transcripts.

Supplemental Figure 3. A mutation affecting the function of the pre-TCR prevents the pathological effects of the LAT Y136F mutation. The LAT^{Y136F} allele was bred on a CD3-ε-deficient (CD3-ε$^{\Delta 5}$) background to generate mice of CD3-ε$^{\Delta 5}$ x LAT^{Y136F} genotype. Thymocytes and splenocytes from wild-type, CD3-ε$^{\Delta 5}$, LAT^{Y136F}, and CD3-ε$^{\Delta 5}$ x LAT^{Y136F} mice at 6 weeks of age, were analyzed for the expression of CD4 versus CD8 and of CD4 versus CD25. The percentage of cells found in each window is indicated and the total numbers of cells found in each organ indicated above the corresponding dot-plots. Eosinophils were found in LAT^{Y136F} thymi and excluded from the analysis using side scatter/forward scatter dot plots.

Supplemental Figure 4. The simultaneous lack of MHC class I and MHC class II molecules prevents the pathological effects of the LAT Y^{136F} mutation. The LAT^{Y136F} allele was bred on an MHC class I- and MHC class II- deficient (MHC KO) background to generate mice of MHC KO x LAT^{Y136F} genotype. Dot plots show the CD4 vs CD8 and CD4 vs CD5 profiles of thymic and splenic cells from wild-type, MHC KO and LAT^{Y136F} x MHC KO mice at 6 weeks of age. Eosinophils were only found in LAT^{Y136F} thymi and excluded from the analysis using side scatter/forward scatter dot plots. The percentage of cells found in each window is indicated and the total numbers of cells found in each organ and averaged from 3 mice showed above the corresponding dot plots.

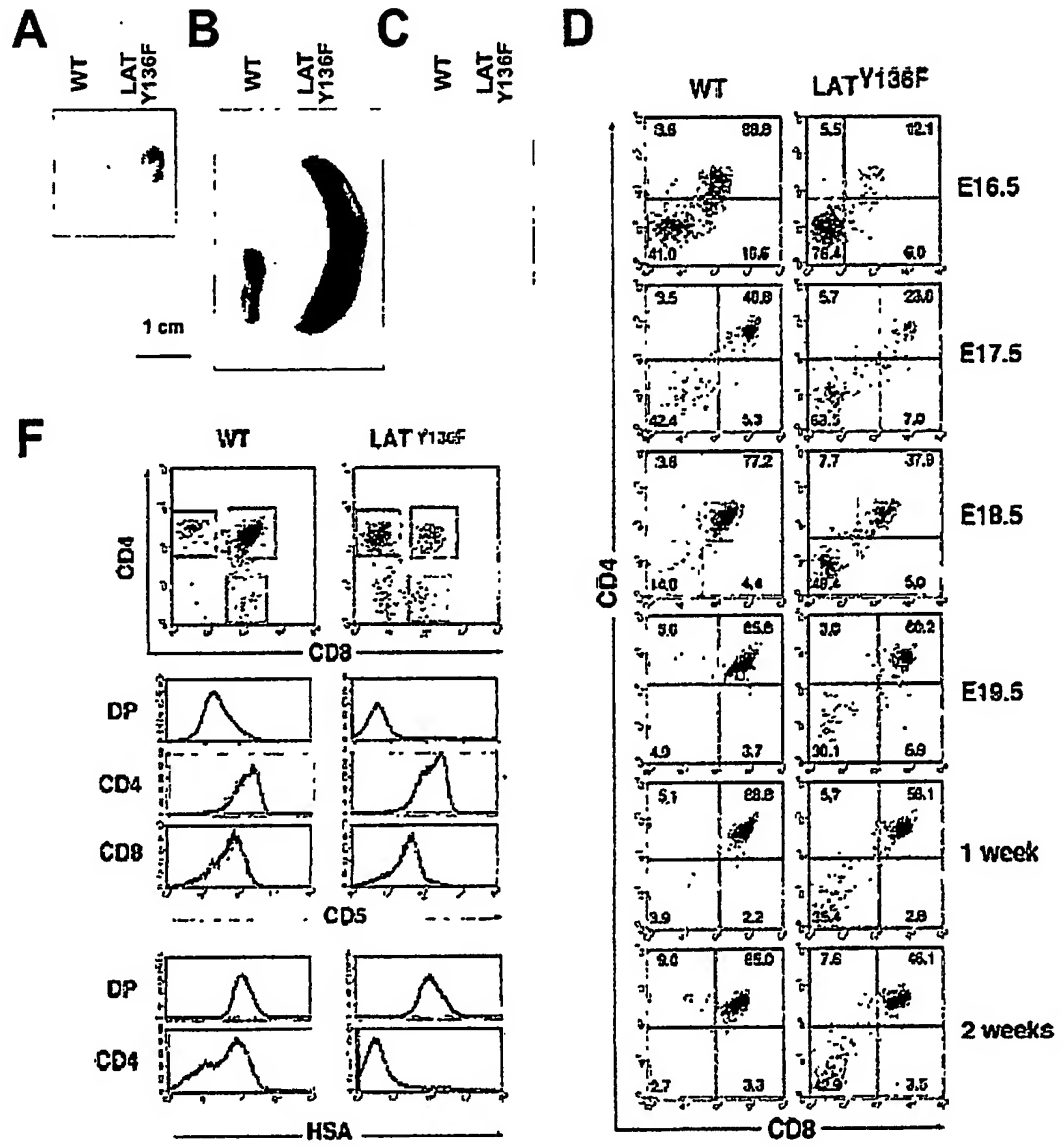

Aguado et al Figure1

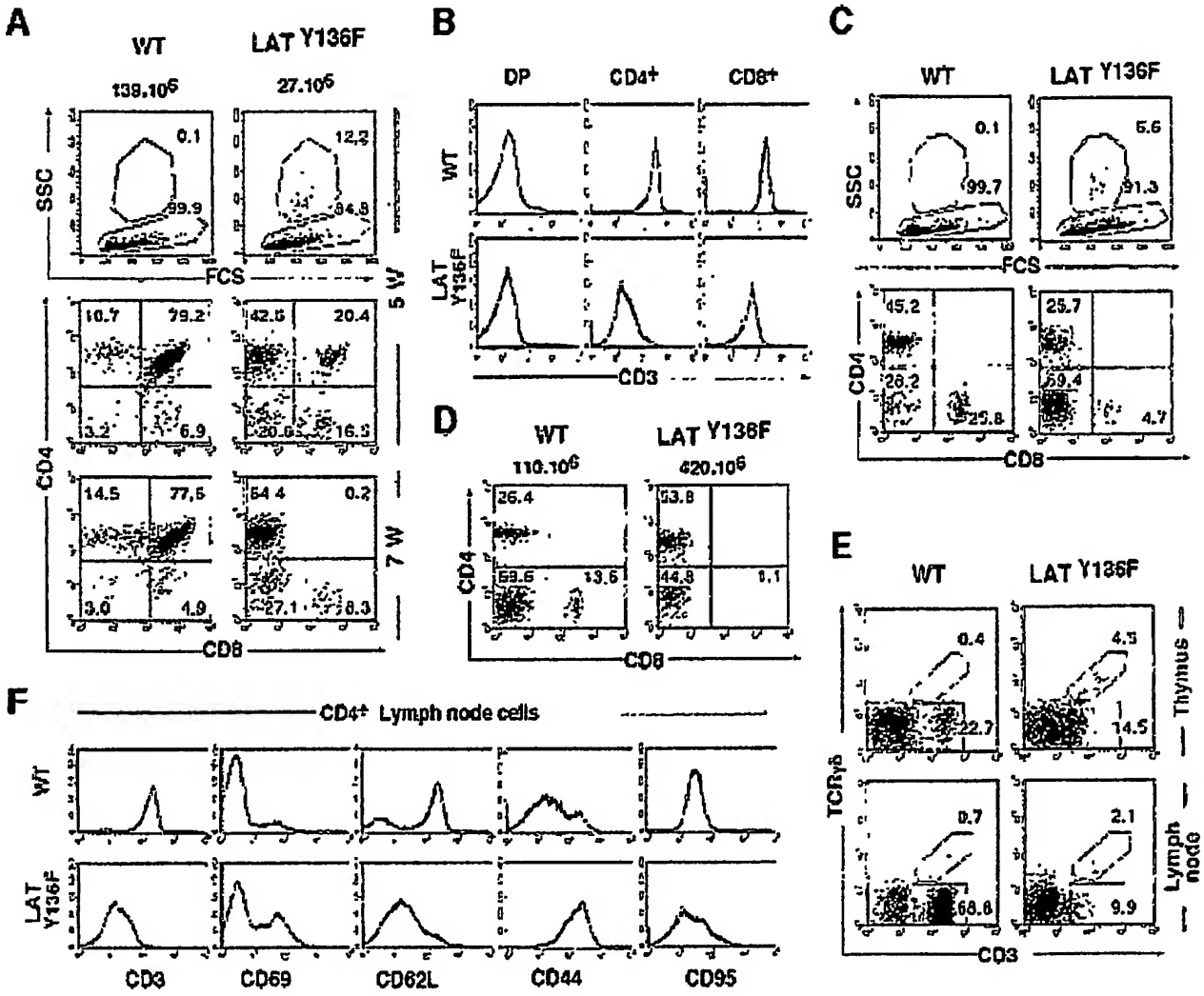

Aguado et al: Figure 2

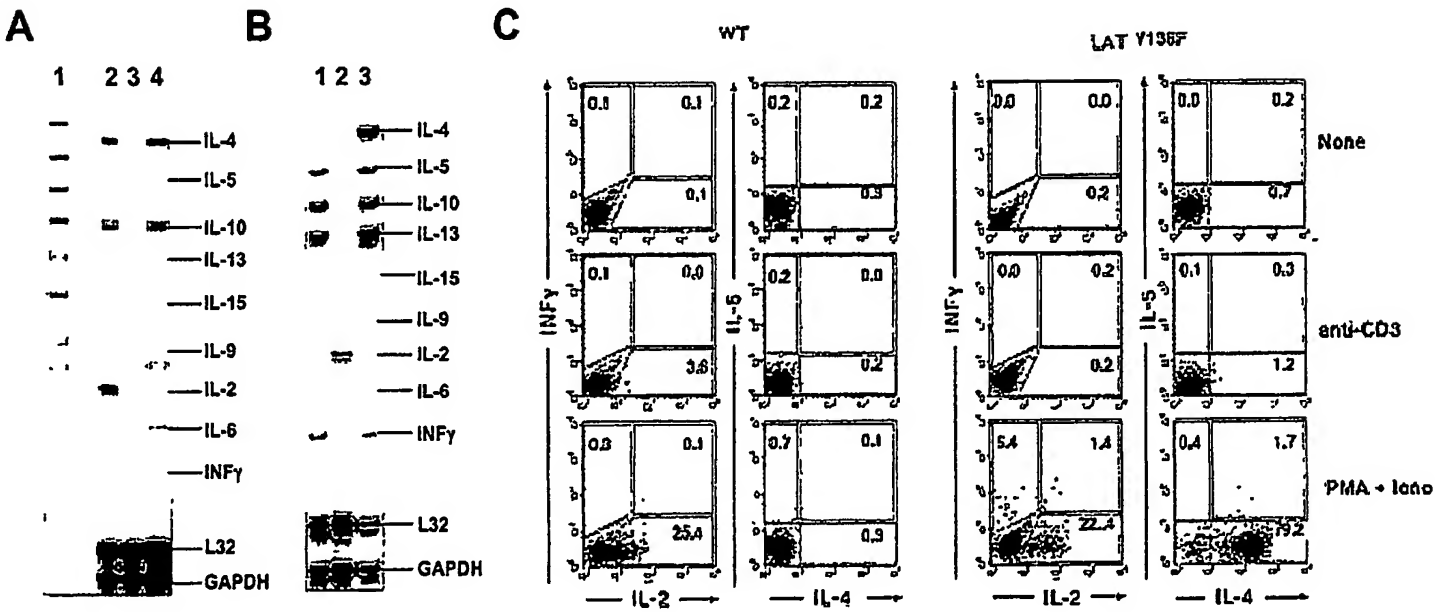

Aguado et al: Figure 3

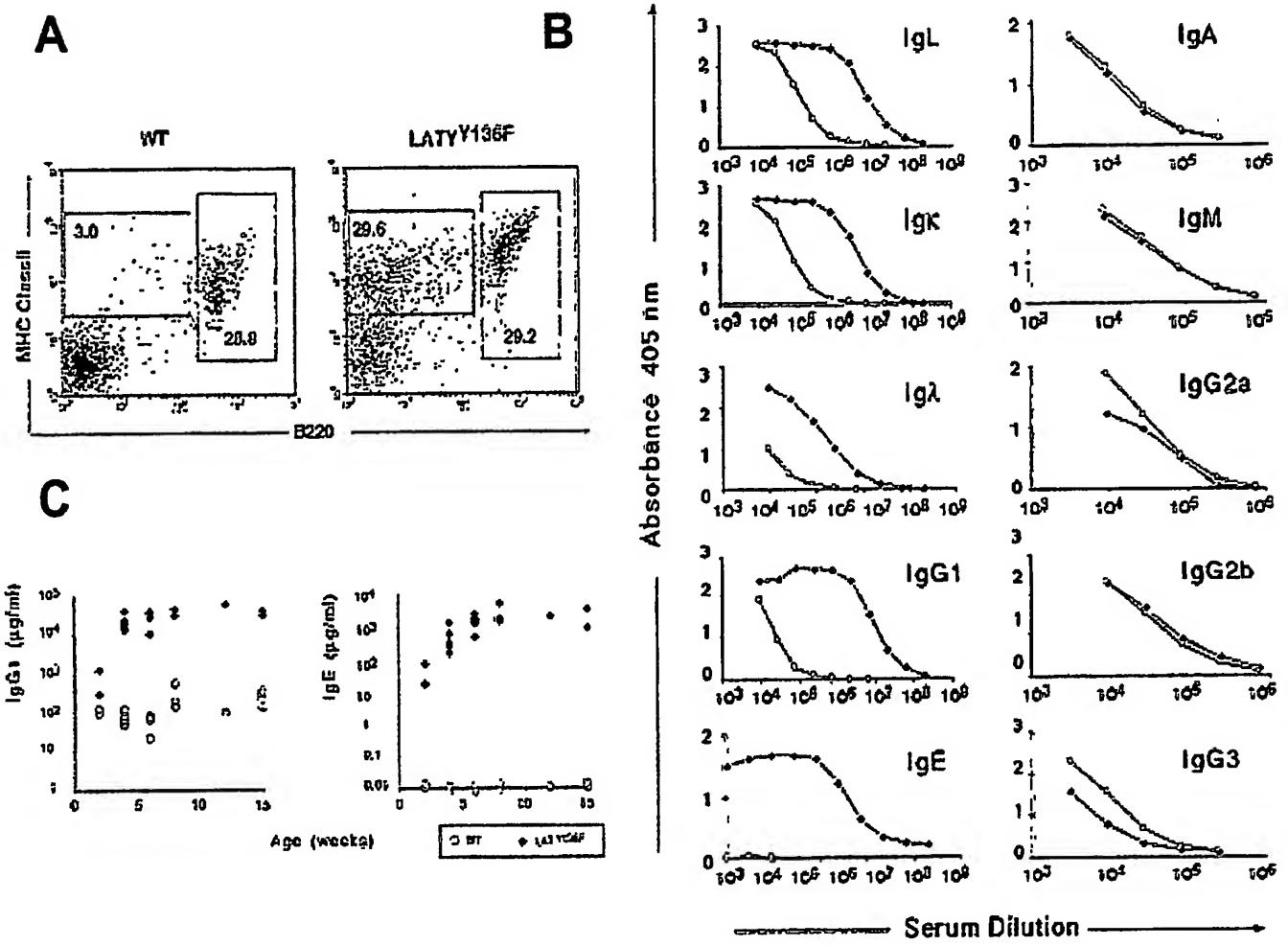

Aguado et al: Figure 4

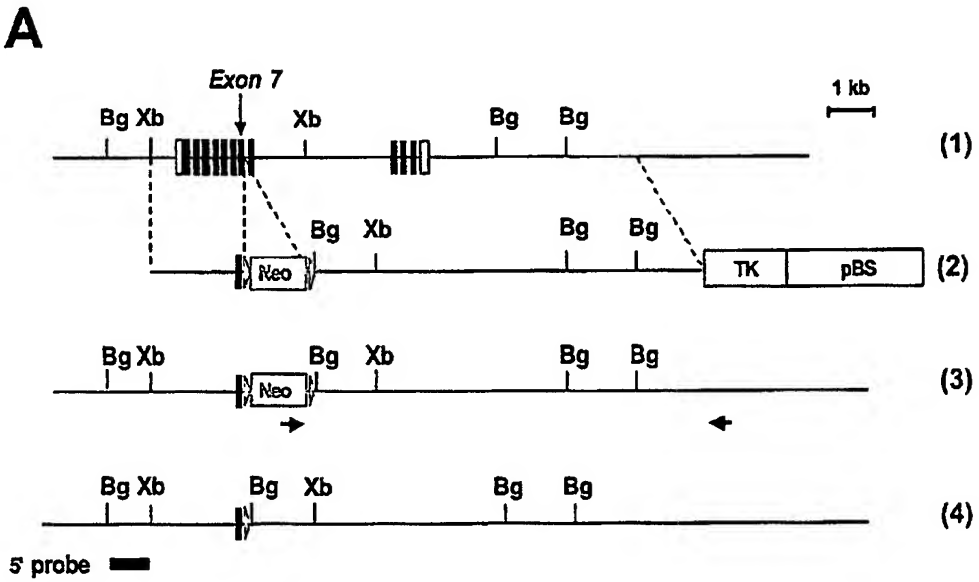

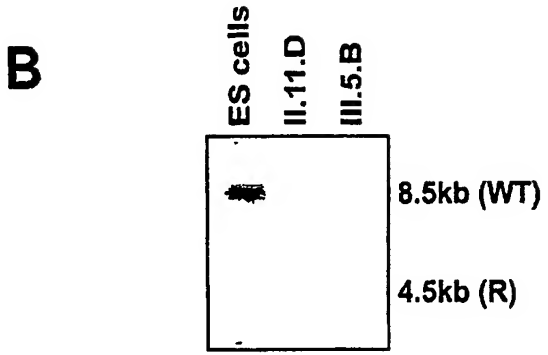

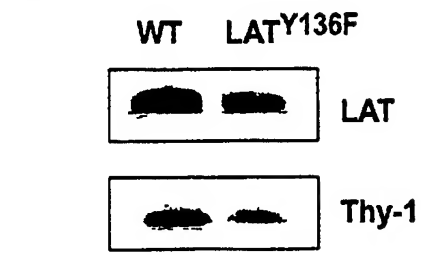

Aguado et al: Supplemental Figure 1

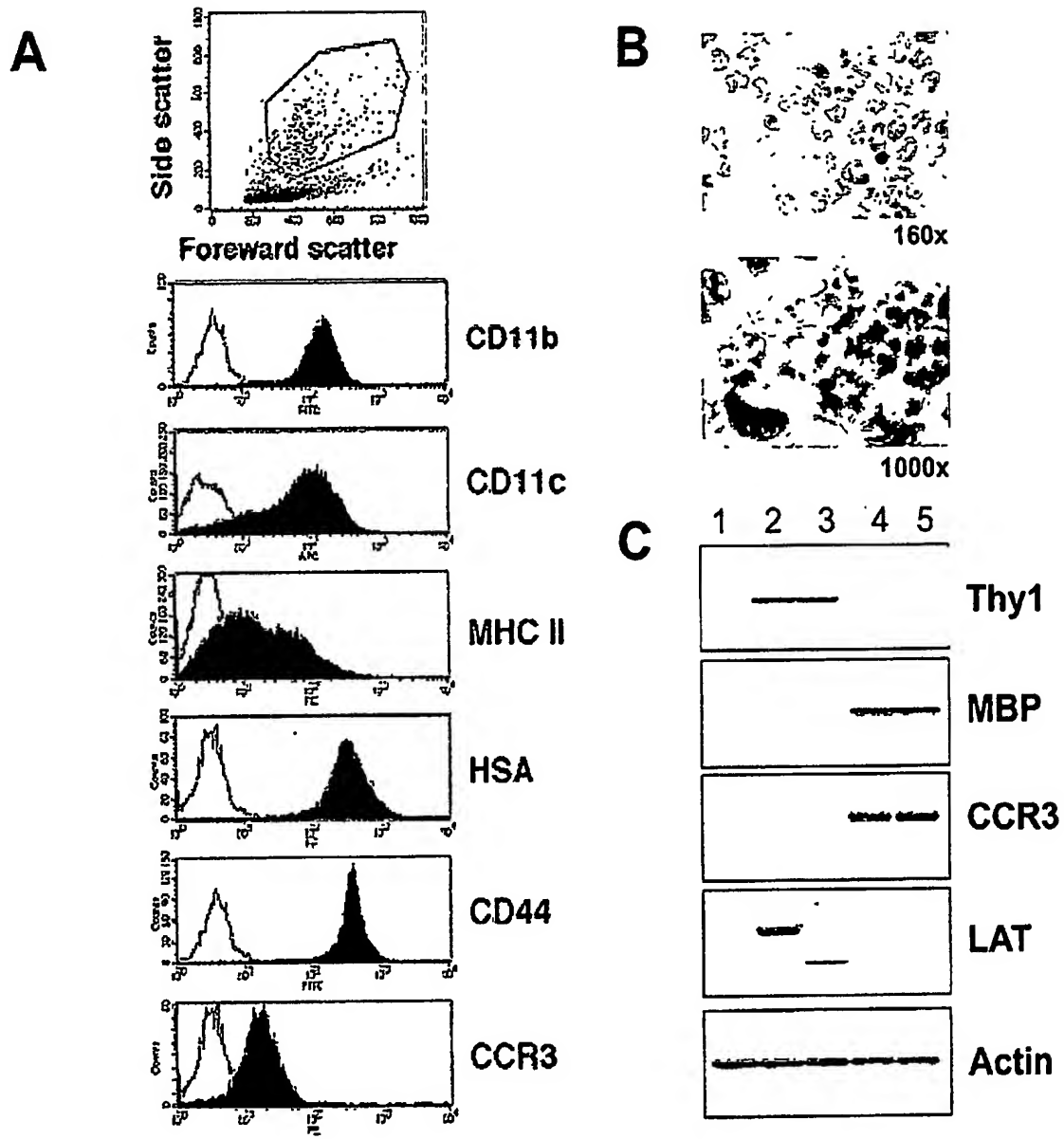

Aguado et al: Supplemental Figure 2

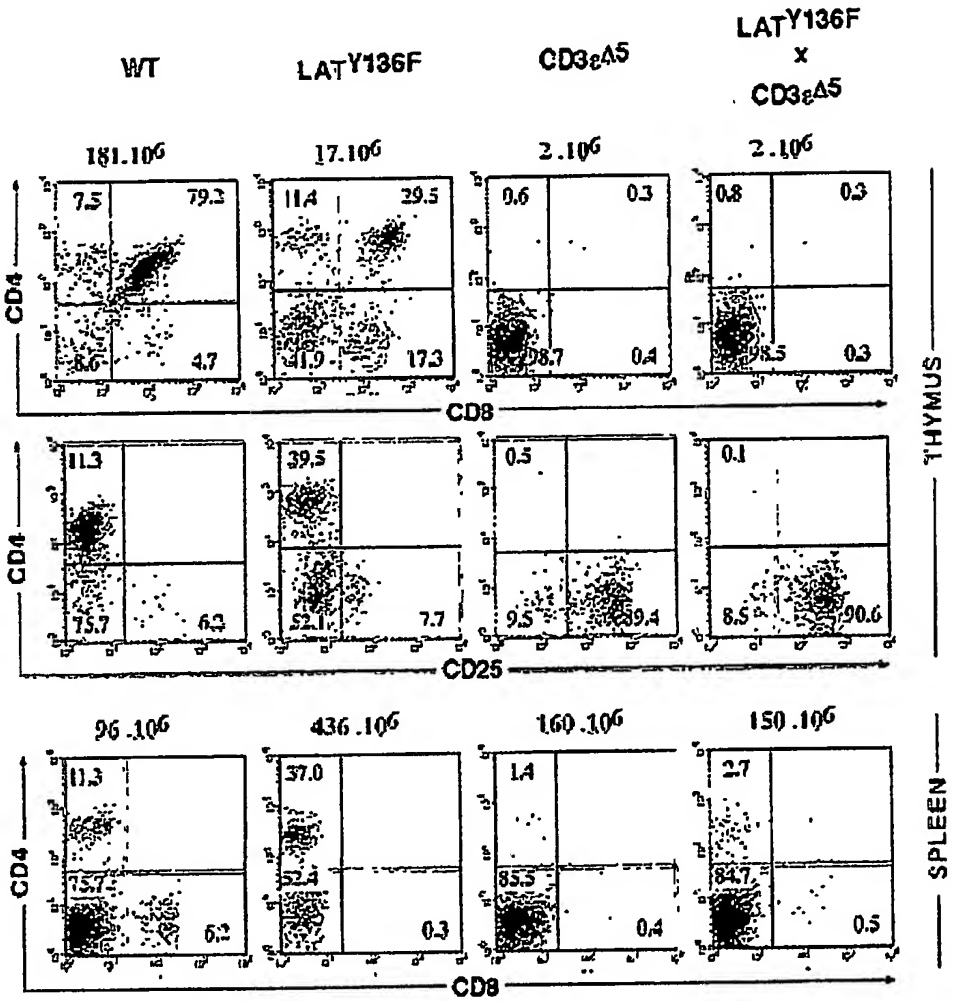

Aguado et al: Supplemental Figure 3

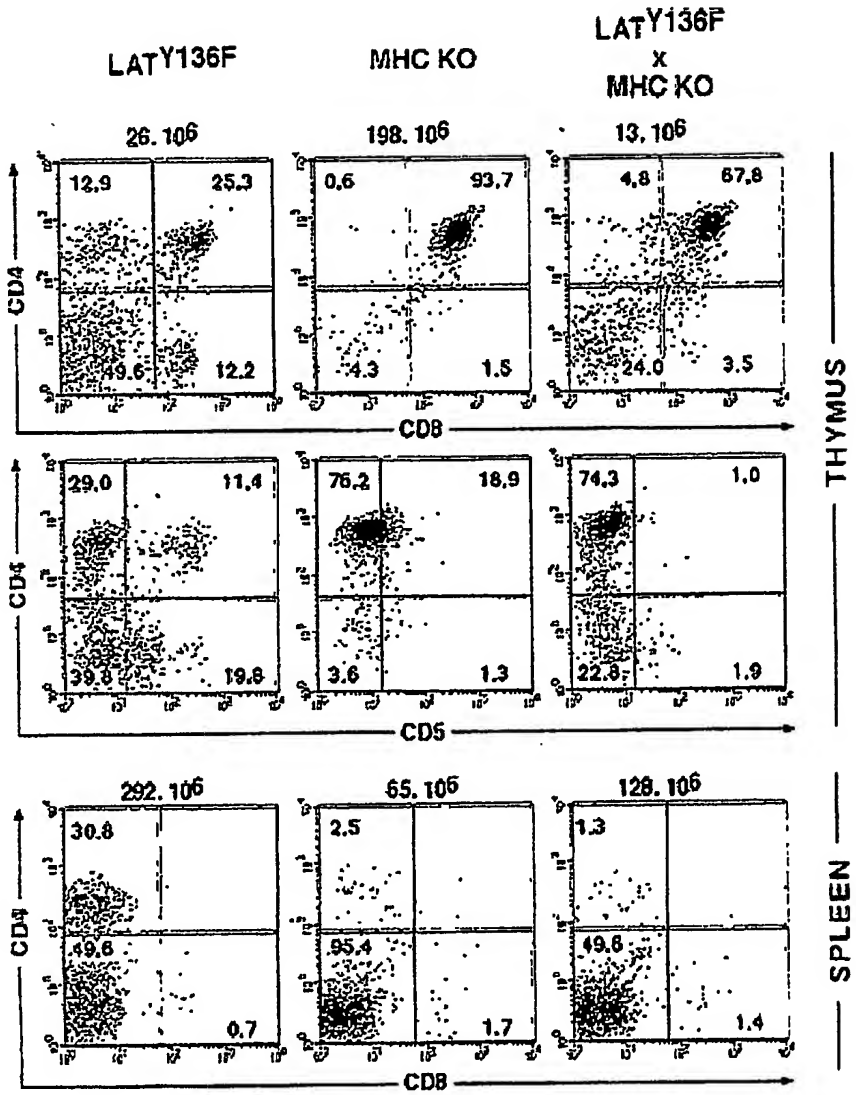

Aguado et al: Supplemental Figure 4